Spatially Resolved Flow-Induced Crystallization Precursors in Isotactic Polystyrene by Simultaneous Small- and Wide-Angle X-ray Microdiffraction

Mari-Cruz García Gutiérrez,*,†,§ Giovanni C. Alfonso,‡ Christian Riekel,† and Fiorenza Azzurri‡

European Synchrotron Radiation Facility, BP 220, F-38043 Grenoble Cedex, France, and Department of Chemistry and Industrial Chemistry, University of Genoa, 16146 Genoa, Italy

Received July 17, 2003; Revised Manuscript Received September 29, 2003

ABSTRACT: The structural and morphological evolution of shear-induced crystallization precursors generated by pulling a single fiber through a thin layer of molten isotactic polystyrene (i-PS) has been spatially resolved by simultaneous small- and wide-angle X-ray microdiffraction in samples with different thermomechanical histories. Frozen precursor structures with shish-kebab morphology have been detected at different levels of evolution during early stages of their formation, the first step being the development of bundles of few parallel chains oriented along the flow direction (shish) followed by the growth of layered lamellar assemblies (kebabs) simultaneously to the appearance of a very weak wide-angle X-ray diffraction (WAXS) signal corresponding to a crystallinity index lower than 1%. A high degree of orientation of the ordered precursors has been found in the polymer matrix at very close distance from the fiber surface when the sample is quenched to room temperature immediately after cessation of flow; much lower crystal orientation has been detected when the sample was left to crystallize during some time at 180 °C before quenching to below T_g. Competition between relaxation and crystallization leads to destruction of the smallest and less oriented precursors, while new crystallites with a slightly different orientation are generated. The experimental evidences are consistent with the existence of quasi-ordered clusters in the melt whose size and orientation distributions are dictated by characteristics of the flow field.

Introduction

Formation of nuclei precursors in sheared melts of crystallizable polymer has mainly been inferred from the indirect observation of very fast crystallization kinetics[1−4] and highly enhanced nucleation density appearing in samples submitted to flow just before,[5,6] or during,[7] solidification. Recently, some direct observation of alteration in the small-angle X-ray scattering profiles of sheared i-PP melts has been reported by Somani et al.[8] Furthermore, Li and de Jeu[9] have found evidences of smectic bundles in step-sheared undercooled i-PP and suggested that these oriented pseudo-ordered aggregates provide nucleation sites for epitaxial growth of folded chain lamellae. The last experiments also indicate that the flow-induced bundlelike aggregates of locally parallelized chain segments are probably metastable structures. Also, rheo-Raman studies of moderately sheared PE melts suggest flow-induced formation of short all-trans sequences, whose likelihood increases on increasing shear rate and that, just above the melting temperature, can linger for several hours after cessation of shear.[10] The formation of precrystalline assemblies, preceding development of stable crystals and constituting a favorable pathway to crystallization, has also been proved in low molecular weight substances by in-situ SAXS and WAXS.[11]

From experiments in which a very intense and highly localized shear flow field is obtained by pulling a single fiber through a thin layer of molten polymer, it has been shown that the flow-induced structures, acting as predetermined crystallization nuclei when the system is brought to below melting temperature, slowly relax upon cessation of the flow, with gradual recovery of the equilibrium situation of the unperturbed melt.[12] In qualitative terms, all the above experiments evidences are well explained by a model of flow-induced production of athermal nuclei which, on the basis of sound thermodynamic principles, enables one to capture the essential features of the early stages of the phenomenon.[13]

Scanning X-ray microdiffraction with beam sizes of a few micrometers[14] allows one to obtain high-quality simultaneous WAXS and SAXS patterns while accurately mapping the region of interest in the samples. The goal of the present study is to investigate the perturbed zone around the pulled fiber to obtain information from microvolume elements of well-known thermal and flow history and hence to spatially resolve the features of precursor structures along the shear rate gradient perpendicular to the fiber axis as well as their evolution upon cooling and crystallization.

Experimental Section

Materials and Methods. Isotactic polystyrene (i-PS) homopolymer with 97% of isotactic dyads, purchased from Polymer Laboratories LTD (UK), was used in this study. The weight-average molar mass and the polydispersity index were $M_w = 939\,000$ and $M_w/M_n = 6.4$, respectively. Samples consist of a single glass fiber, 17 μm diameter, sandwiched between two thin polymer layers (about 100 μm each) and confined between two thin cover glasses.

A simple and effective way to produce a very intense and highly localized shear flow field is to pull a single fiber through a thin layer of molten polymer. According to Monasse,[15] the

† European Synchrotron Radiation Facility.
‡ University of Genoa.
§ Present address: Instituto de Estructura de la Materia, CSIC, Serrano 121, 28006 Madrid, Spain.
* Corresponding author: Tel 34-91 561 68 00; Fax 34-91 564 55 57; e-mail imtc304@iem.cfmac.csic.es.

10.1021/ma0350157 CCC: $27.50
Published on Web 12/17/2003

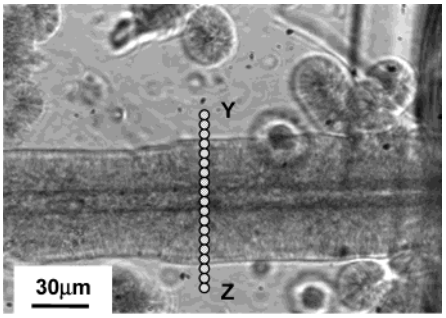

Figure 1. Optical micrograph of a perturbed unrelaxed semicrystalline i-PS sample (sample B), showing schematically a linear raster scan with 5 μm raster increment through the perturbed zone (line YZ). A transcrystalline layer surrounding the fiber all along its length is clearly detected.

intensity of the flow field depends on rate of pulling, geometrical characteristics of the system, and rheological properties of the polymer matrix and rapidly decays with distance from fiber surface (tens of micrometers). A homemade fiber pulling device, enabling us to pull the fiber at constant linear velocity in the range between 0 and 14 mm/s over a distance up to 10 mm, was coupled with a Mettler FP 80 hot stage, to apply flow conditions suitable for the development of oriented nucleation precursors.

Samples were initially brought to a temperature of 260 °C for 5 min to relax occasional stresses due to sample preparation. At this temperature, the fiber was pulled for 2 s at a rate of 5 mm/s before submitting the sample to different thermal histories. Under these conditions, it is estimated[15] that the shear rate at the interface corresponds to about 10^3 s^{-1} and that it reduces to below 20 s^{-1} at a distance of about 20 μm from the fiber surface. Three samples were investigated: two of them were quenched in air at 20 °C directly from 260 °C; for the third one, an intermediate crystallization step at 180 °C, at which i-PS exhibits its maximum crystal growth rate,[16,17] was applied before quenching. The following thermomechanical histories were applied: (i) Sheared unrelaxed amorphous-like sample (sample A): this sample was quenched to room temperature immediately after cessation of flow. (ii) Sheared unrelaxed semicrystalline sample (sample B): this sample was quickly transferred into a hot stage set at 180 °C where it was held for 90 min to crystallize just after the pulling stage. Afterward, quenching in room temperature air was performed. (iii) Sheared and relaxed amorphous sample (sample C): before quenching to room temperature, this sample was held 40 min at 260 °C to relax the perturbation produced by pulling the fiber.

X-ray Microdiffraction. X-ray diffraction experiments were performed at the European Synchrotron Radiation Facility (ESRF) microfocus beamline (ID13) using a wavelength λ = 0.097 55 nm (Si-111 monochromator) and a 5 μm diameter beam from a post-collimator.[14] Diffraction patterns were recorded with a CCD detector with 130 mm converter screen (MAR; 64.45 × 64.45 μm^2 pixels; 16-bit readout). Simultaneous μWAXS and μSAXS experiments were performed. The sample-to-detector distance was calibrated by an Ag−behenate sample as D = 157.59 mm. The lower limit in q ($q = 4\pi \sin\theta/\lambda$) was q_{min} = 0.07 nm^{-1}. Typical recording times were 30 s. Experiments were performed in air at T = 25 °C.

The sample was aligned on a goniometer head so that the glass fiber was nearly horizontal (Figure 1). A specific point of the sample was selected by a microscope and then transferred into the center of the X-ray beam at the exit of the collimator by a three-axis gantry, which was interfaced by a computer-controlled motion software.[14] The sample was scanned through the beam along the line YZ (Figure 1) with 5 μm steps. At every position a diffraction pattern was recorded in transmission. For background correction a pattern without sample was recorded. Data analysis was performed with the FIT2D software package.[18]

Results

Simultaneous μSAXS and μWAXS. As has been pointed out previously, three samples with different thermomechanical histories have been investigated. Preliminary observations by polarized optical microscopy evidenced that only in sample B a cylindritic morphology is generated around the fiber, and some spherulites grow in the unperturbed regions far from fiber surface (Figure 1). The other types of samples were lacking of any evident morphological feature at any location; only a faint birefringence was found in sample A at the fiber−matrix interface.

The small X-ray beam divergence of about 0.2 × 0.2 $mrad^2$ allowed us to record both the WAXS and SAXS signals together in the same pattern and therefore to perform an easier and more accurate data analysis.

1. Sheared Unrelaxed Amorphous-like Sample. Figure 2 (top) shows a series of WAXS patterns, obtained at distances of 5 μm one from another, that provides a detailed map across the region from the fiber surface (Figure 2a) to the unperturbed zone (Figure 2f). Three weak crystal reflections are observed in WAXS patterns of Figure 2a−e (very faint in Figure 2e) while no crystalline reflection is detected in Figure 2f, which corresponds to the unperturbed zone. The three reflections appearing in the WAXS patterns of Figure 2a−e are sharp and have narrow azimuthal width, which indicates presence of highly oriented i-PS crystals with good crystalline register. To index the crystal reflections, the intensity of the WAXS pattern of Figure 2c was radially integrated and the 1-D intensity profile (Figure 2, bottom) fitted using an amorphous halo, obtained from a pattern that does not show any crystalline reflections, and three Gaussian functions for the crystalline peaks. Analysis of the fitted profile allowed us to index the three weak peaks as the 220, 211, and 012 reflections corresponding to the trigonal unit cell (a = b = 2.19 nm and c = 0.67 nm) of i-PS.[19]

The central part of diffraction patterns shown in Figure 2 has been magnified in order to observe the SAXS signal. The results are shown in the upper part of Figure 3, together with two further patterns collected at larger distance from the fiber (patterns g and h). The SAXS obtained at positions where the WAXS gives evidence of crystalline peaks (Figure 3a−e) exhibit both equatorial and meridian maxima; on the other hand, the pattern taken 5 μm further away from the fiber (Figure 3f) only shows a weak equatorial maximum while those taken even further (Figure 3g,h) only show a very weak isotropic scattered intensity with no detectable maximum. Both equatorial and meridian maxima become weaker with increasing distance from the pulled fiber, indicating that, in the adopted conditions, the structuring effects of the flow field vanishes at about 30 μm from the fiber surface. The equatorial maximum can be attributed to bundles of parallel chain segments preferentially oriented along the flow direction (shish structures) while the meridian maximum observed at positions close to the fiber surface, where the flow field is more intense, is consistent with presence of layered lamellar assemblies (kebab) growing epitaxially from the shish structures in a direction perpendicular to their axis.[20,21] The 1D SAXS intensity profiles (Iq vs q) along the equator corresponding to Figure 3a−e are shown in the plot of the same figure.

2. Sheared Unrelaxed Semicrystalline Sample. In Figure 4, a series of WAXS patterns obtained as in

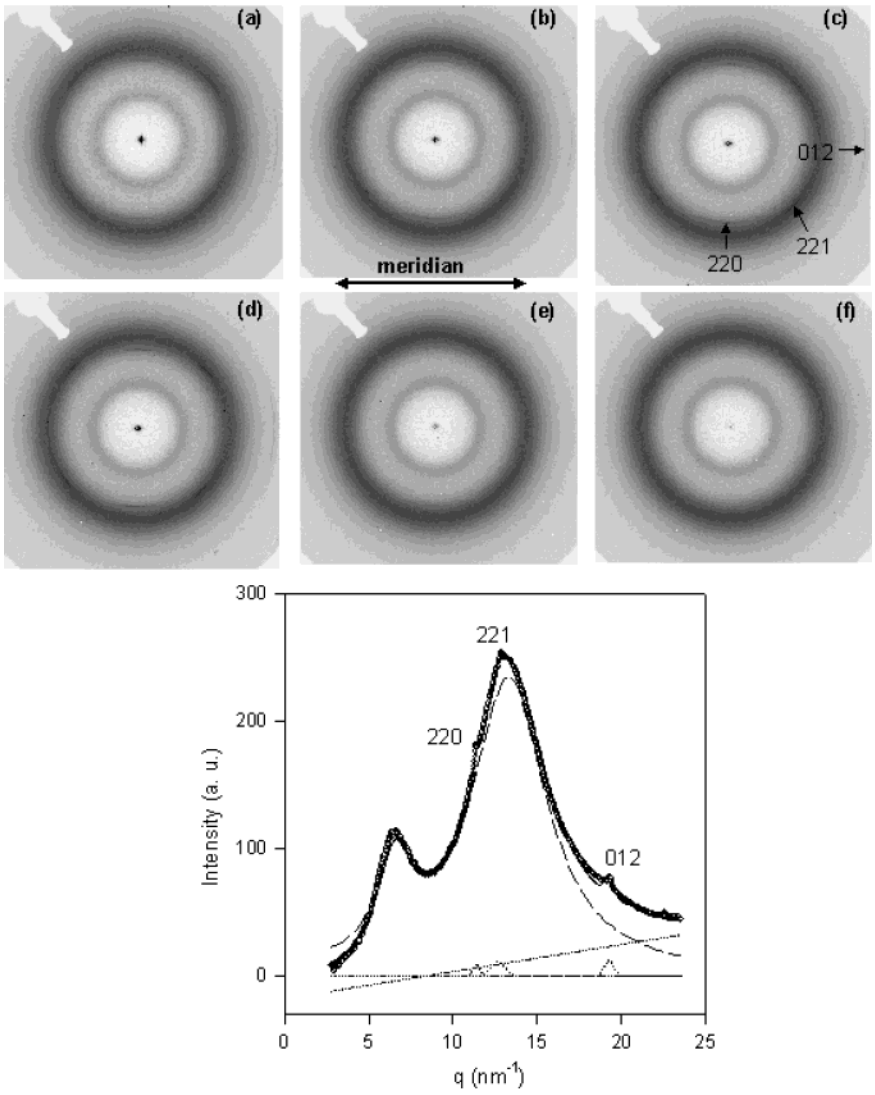

Figure 2. WAXS patterns recorded mapping the perturbed region of sample A, with steps of 5 μm, from the fiber (a) to the unperturbed region (f), (top). Radial profile of pattern (c) showing the peak deconvolution analysis to separate the crystal reflections and the amorphous halo (bottom).

Figure 2 are reported for the sample that was held to crystallization at 180 °C for 90 min before quenching below T_g. In addition to the three weak crystal reflections already observed in sample A, new reflections, indexed as 110, 300, 410, and 330 according to the trigonal unit cell of i-PS,[19] are detected in the patterns of Figure 4a−e. The crystal reflections of this sample are stronger and exhibit a broader azimuthal width than those detected in sample A; this indicates a lower level of orientation of i-PS crystals in sample B than in sample A.

Both an equatorial streak and a very well defined two-lobe meridian pattern are observed in Figure 5a, in which the SAXS corresponding to the position closest to the fiber is shown. In this partially crystallized sample, the meridian lobes do not change appreciably throughout the transcrystalline layer, while the equatorial streak rapidly vanishes with increasing the distance from the fiber surface (Figure 5b,c). This feature is parallel to the observation that WAXS reflections in sample B are broader than in sample A and further demonstrates a lower degree of chain orientation.

3. Sheared Relaxed Amorphous Sample. The simultaneously acquired WAXS and SAXS patterns obtained by sampling microvolumes of the relaxed sample at the fiber−matrix interface and 5 μm apart are shown in parts a and b of Figure 6, respectively. No reflection characteristic of crystalline order is observed in either WAXS patterns. Similarly, the SAXS pattern at 5 μm from the fiber does not show any variation with the azimuthal angle; however, when the fiber−matrix interface is sampled, a faint and very narrow equatorial streak, which can be attributed to a refraction effect, appears in the pattern (Figure 6a, bottom). It should be noted that this pattern is substantially different from those corresponding to the interface of samples A and B, in which the equatorial scattered intensity is composed by a broad maximum (shish) and a narrow streak (refraction).

Discussion

Gradient of Precursor Structures in the Perturbed Region. The results described above indicate that, provided the intensity of the flow field is sufficiently large, precursors of nuclei with shish-kebab type morphology form under shear flow also at temperatures above the equilibrium melting point. This is in

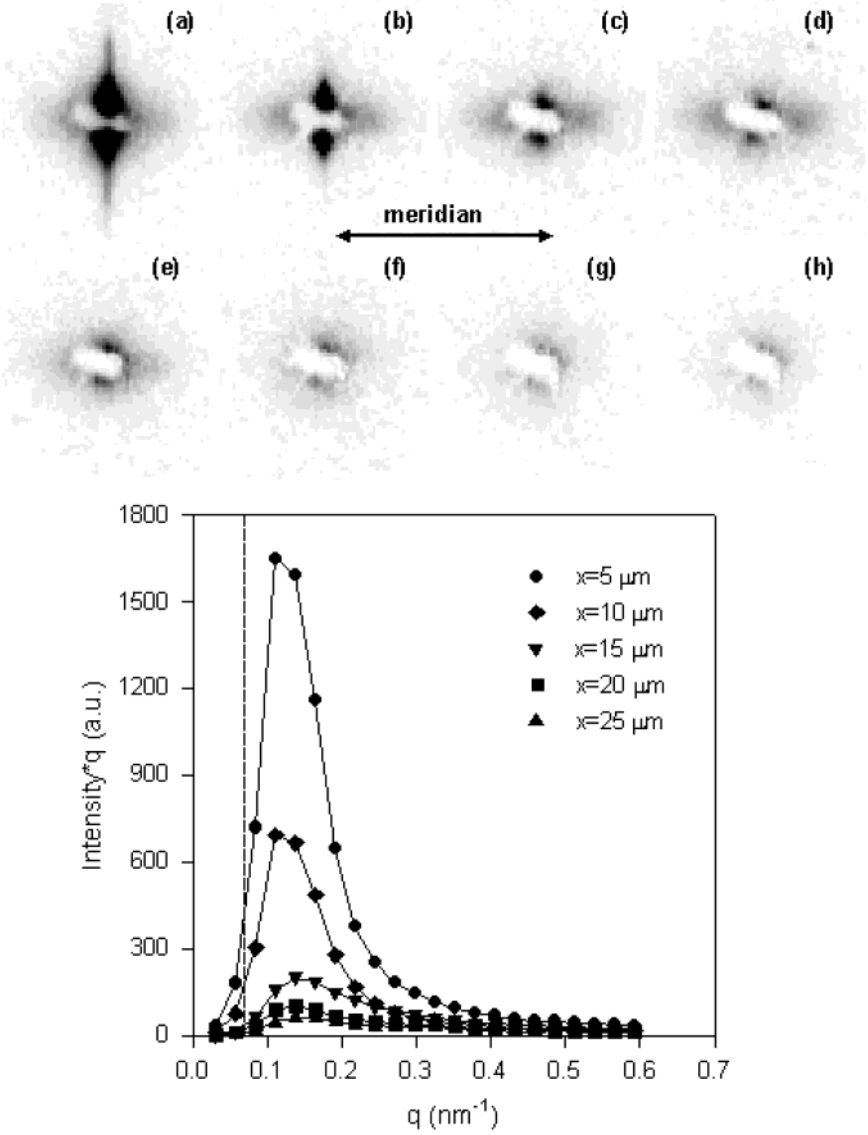

Figure 3. SAXS patterns recorded simultaneously to WAXS patterns shown in Figure 2 (top). SAXS intensity profiles (Iq vs q) along the equator (bottom); the dashed line corresponds to the resolution limit $q_{min} = 0.07$ nm^{-1}.

agreement with what has been observed by Samon et al.[20] from in-situ X-ray studies of fiber spinning and by Somani et al.[21] in their in-situ rheo-SAXS and rheo-WAXS investigations**.** Results are also consistent with above authors and the recent suggestion of Li and de Jeu[9] that at the very early stages of crystallization the shish are mostly mesomorphic with only a small crystalline fraction.

Thanks to the very slow crystallization kinetics of i-PS,[16,17] in the present investigation it has been possible to detect features of the structures produced by shear flow of different intensity and frozen at different stages of their evolution. As the intensity of the flow field increases moving toward the fiber, also the concentration of precursors increases. This is shown in Figure 7, in which the integrated equatorial intensity (I_{shish}), calculated from the area under the 1D SAXS equatorial profiles, is plotted as a function of distance from the fiber. In this figure it is also illustrated the steep decrease of shear rate in the direction perpendicular to the flow, i.e. to fiber axis. The two plotted lines have been calculated from the equation proposed by Monasse[15] with two different values for the exponent of the rheological power law equation, n

$$\dot{\gamma}(r) = \frac{1-n}{n}\frac{1}{r^{1/n}}\left[\frac{1}{r_f^{(n-1)/n} - r_e^{(n-1)/n}}\right]V_f \qquad (1)$$

r_f is the fiber radius, r_e the half-thickness of the polymer film, V_f the pulling rate of the fiber, and r the distance from the fiber axis. The strict correlation between the decay of concentration of precursors and of shear rate is straightforward and proves that the intensity of flow is a key experimental variable in the formation of the ordered nanostructures from which crystals develop on subsequent cooling.

Also, the geometrical characteristics of the large and oriented clusters are dependent on the local velocity gradient. Figure 8 shows that the average periodicity of shish structures (intershish distance, from center to center) perpendicular to flow direction (W_{shish}), calculated from the peak position in Figure 3 (bottom), appreciably increases with decreasing distance from the fiber. By considering the shishs as high electron density

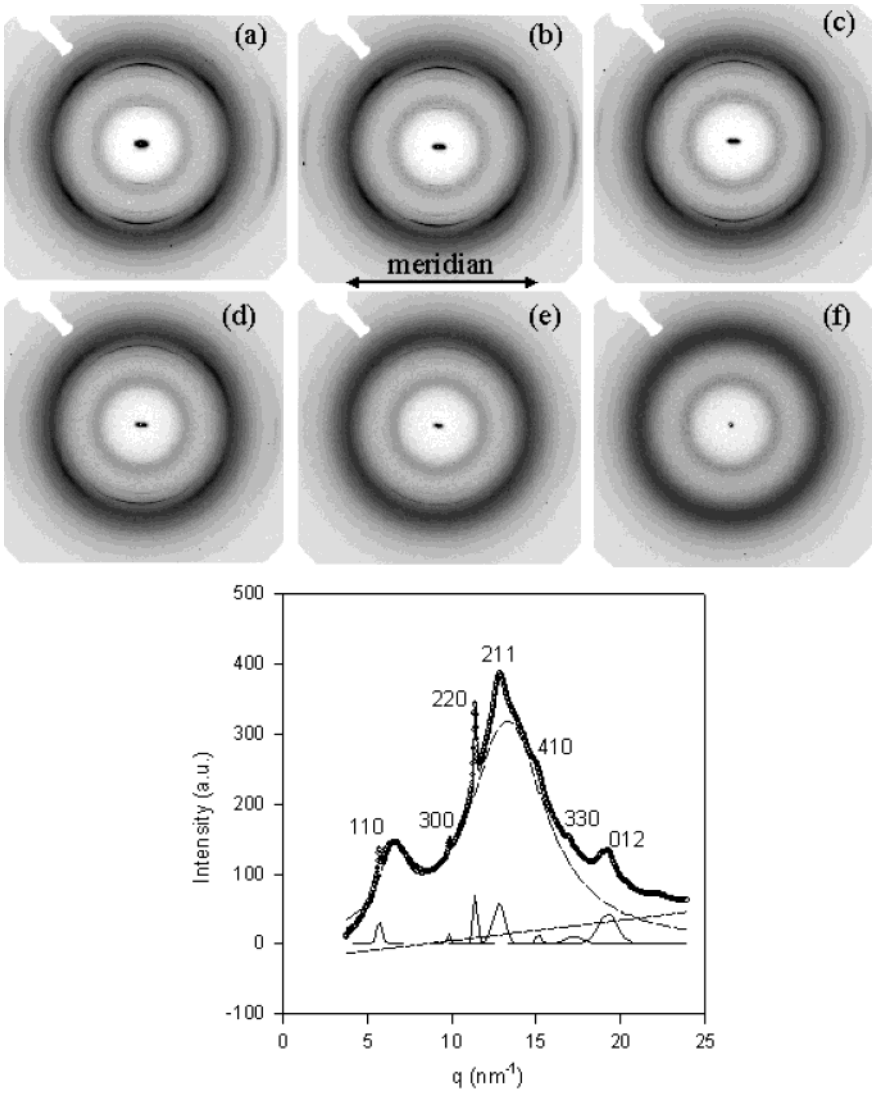

Figure 4. Series of WAXS patterns mapping the perturbed region of sample B and recorded with steps of 5 μm from the fiber to the position Z in Figure 1 (top). Radial profile of pattern (a) showing the indexes of crystal reflections (bottom).

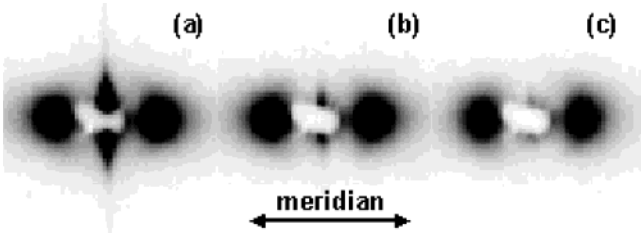

Figure 5. SAXS patterns recorded simultaneously to the WAXS patterns shown in Figure 4 (top) at the positions a−c.

structures (close to the crystal density) imbedded in a low density barely oriented amorphous phase, the emerging picture of the superstructural organization produced under the effect of high shear flow fields is that of a pseudo-two-phase system in which cylindrical aggregates of asymmetric units (chain segments) are spontaneously formed. On the basis of thermodynamic arguments,[13] it is expected that the volume of these cylindrical precursors increases with increasing the intensity of flow. Since the thermodynamically optimum shape of these cylinders corresponds to minimum surface energy and it is characterized by a constant axial ratio (L_{shish}/R_{shish}) whose value is dictated by the end and lateral surface free energies, the decrease of W_{shish} with distance from fiber surface can be justified. At low shear rates, relatively far from the fiber surface, many small (short and thin) and closely spaced bundles of aligned chain segments are generated; on increasing the intensity of the flow field the length of stretched threads increases, and larger domains, also formed by association of the smaller ones thanks to the action of tie chains connecting adjacent bundles, are stabilized in a matrix of unoriented or slightly oriented elements. In close proximity to the fiber, where the shear rate is higher, the lateral size of highly oriented structures further increases at the expenses of the interposed chain segments.

The kebabs develop perpendicular to the shish in the early stages of growth. The diffracted intensity related to the presence of layered structures increases with increasing the intensity of the flow field as is illustrated in Figure 9, where the integrated meridian intensity (I_{kebab}) is plotted as a function of the distance from the axis of the pulled fiber. By comparing Figures 9 and 10, one observes that the WAXS crystalline reflections appear at the positions in the sample where the SAXS signal associated with the kebabs is also detected. In addition, the dependence of I_{kebab} on the distance from the pulled fiber (Figure 9) is similar to that of the degree

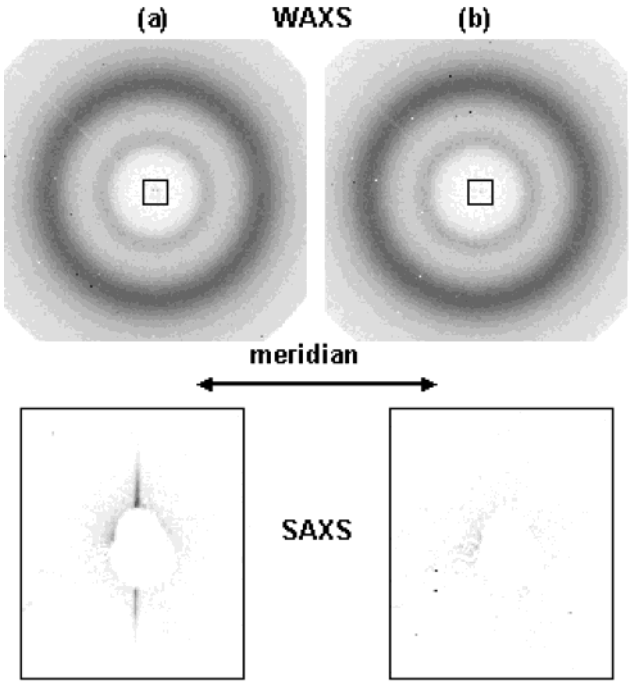

Figure 6. Simultaneous WAXS and SAXS patterns recorded at the fiber−matrix interface (a) and 5 μm apart (b).

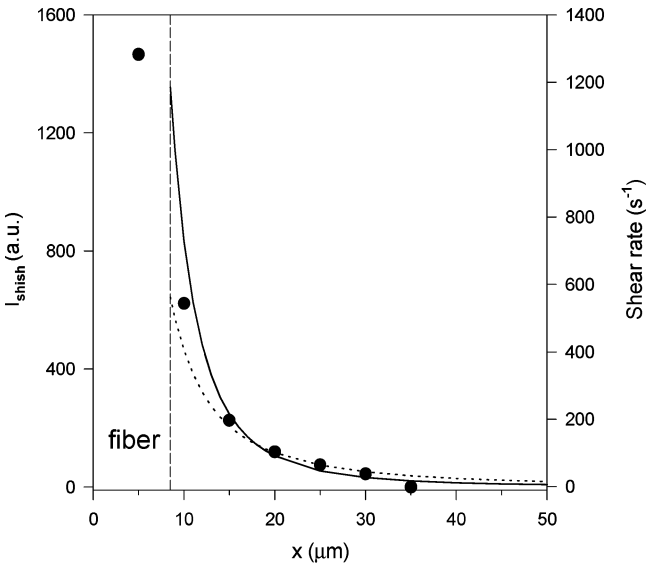

Figure 7. Plot of integrated intensities of the SAXS equatorial maximum (I_{shish}) vs position from the center of the pulled fiber in sample A. The two lines correspond to shear rates calculated according to Monasse's eq 15 and assuming the pseudoplasticity index equal to 0.5 (solid line) and 0.33 (dashed line). The fiber−matrix boundary is indicated by the broken line.

of crystallinity (Figure 10) calculated from the equation $X_c = \sum I_c/\sum(I_a + I_c)$, where I_c is the integrated area underneath the crystalline peaks and I_a is the integrated area of the amorphous halo, estimated by the previously described peak-fitting procedure of the integrated WAXS intensity as shown in Figure 2 (note that the degree of crystallinity calculated for positions 5 and 10 μm from the fiber axis is lower than expected because at those positions the glass fiber is contributing to the amorphous fraction). Both evidences strongly suggest that the layered structures are crystalline. The above results—the appearance of the SAXS equatorial signal before the SAXS meridian and WAXS signals, the very

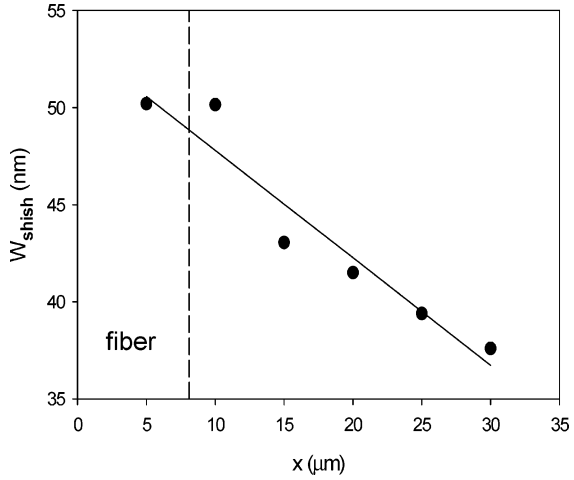

Figure 8. Average periodicity of shish structures (W_{shish}) in sample A as a function of position from the center of the pulled fiber. Experimental data are fitted to a linear function (solid line) only as an eye guide.

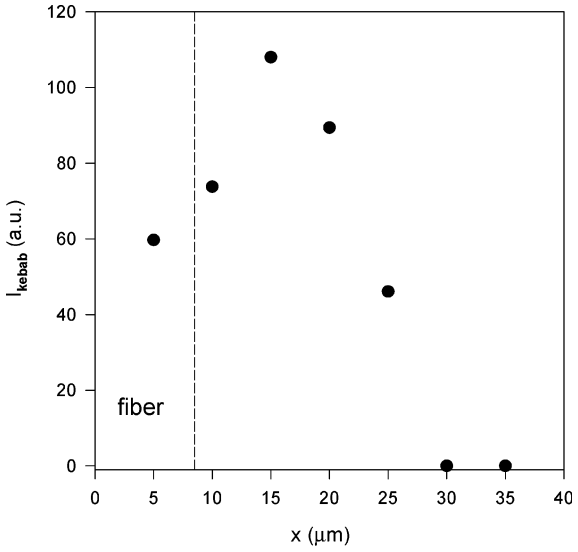

Figure 9. Variation of integrated intensities of the SAXS meridian maximum (I_{kebab}) with distance from the center of the pulled fiber in sample A.

small degree of crystallinity detected (between 0.2 and 0.8%), and the more similar behavior of I_{kebab} to X_c with distance from the pulled fiber than I_{shish}—may suggest that shish structures are mostly mesomorphic with only a small crystalline fraction. This assumption could be in accordance with authors supporting that the shish consists of extended-chain crystals, as it is pointed out in a previous work by Petermann and co-workers on the crystallization study of i-PS from the highly extended melt by TEM,[22,23] where the authors suggest that the initial crystal rods (extended-chain crystals) with diameters of about 11 nm should be surrounded by preordered molecular chains. Hence, the picture proposed concerning the nature of shish structures consists of a very thin core crystal surrounded by polymer chains with mesomorphic order.

The high values of I_{kebab} detected at short distance from the fiber surface in the sample quenched below T_g immediately after fiber pulling are an indication that also the formation of structures responsible of the scattering along the meridian crucially depends on the intensity of the flow field, at short distances from the fiber the density nucleation increases leading to the

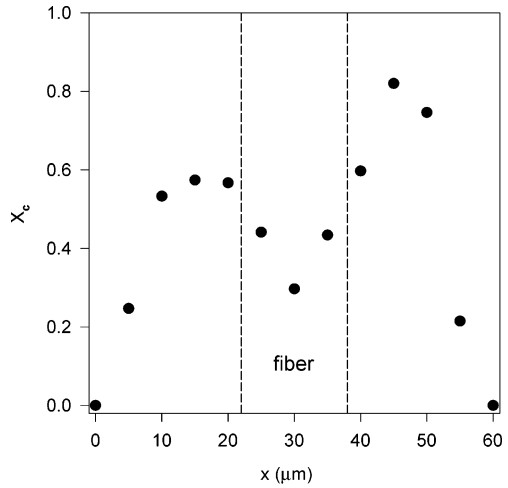

Figure 10. Variation of crystallinity across the perturbed zone in sample A. Note that the maximum attained crystallinity level is below 1%.

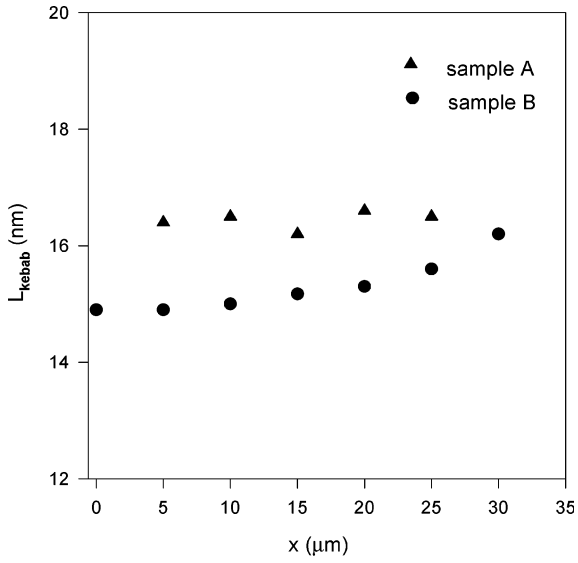

Figure 11. Long period of kebabs (L_{kebab}) in samples A and B as a function of position from the center of the pulled fiber.

growth of more lamellae. Because of the extremely short time the sample has spent in the temperature window in which crystal growth is possible (from ca. 230 to 100 °C), it can be argued that the detected structural features were already existing, under flow conditions, also above the equilibrium melting point of i-PS crystals.[24] Alternatively, one should admit that the enhancement of crystallization rate in the sheared volume is so huge that some crystallinity can develop notwithstanding the very fast quenching to which the sample has been submitted. This seems rather unrealistic in view of the lack of experimental evidences proving that the rate of crystal growth is indeed a sensitive function of segmental orientation.

In sample A, the long period of the layered structures is independent of the sampling position (Figure 11), while in the sample that has been held 90 min at 180 °C, with respect to sample A one observes a clear increase of I_{kebab} and a lower value of L_{kebab} that slightly decreases close to the fiber (Figure 11). This implies that new crystalline lamellae develop at the crystallization temperature also in the volume already containing the flow-induced precursors.

Vanishing Memory of the Effects of Flow on Crystal Nucleation. It is interesting to note that, as was previously pointed out, the WAXS patterns of sample A only show three reflections, corresponding to the 220, 211, and 012 planes of the trigonal unit cell of i-PS (Figure 2), with the 211 and 012 that are stronger than the 220. This situation, corresponding to "row-nucleated" structures, was also found in freeze-dried isotactic polystyrene prepared from a benzene solution,[25] and it is quite different from the common powder WAXS patterns of i-PS, in which additional reflections are present and the two strongest peaks correspond to 220 and 110 planes. Instead, sample B exhibits WAXS patterns that correspond to a morphology intermediate between the highly oriented row-nucleated lamellar layers and the random lamellar orientation found in spherulitic samples. This observation, together with the evidence that in sample B (Figure 5b,c) the intensity of the equatorial streak decreases more rapidly, as a function of the distance from the fiber, than in sample A, suggests that some relaxation of the flow-induced structuring takes place when an intermediate crystallization step is applied in the absence of flow. To this relaxation process should simultaneously involve randomization of chain segments as well as of oriented clusters (shish). All these processes contribute to reduce the concentration of effective crystallization precursors, particularly of the less stable shish, i.e., the smaller and less oriented ones.[13] The disappearance of the barely oriented precursors produced at relatively large distance from the fiber surface (ca. 15−20 μm) explains the sharp decrease of the equatorial scattering found in sample B that has been held for long time above the glass transition temperature. Obviously, also additional random nucleation and crystal growth at 180 °C contribute to the loss of orientation eventually present in the examined samples.

The shish-kebab structures have been generated by the intense local shear flow associated with the fiber pulling at 260 °C, i.e., well above the equilibrium melting temperature of i-PS (T_m^0 = 243 °C).[22] At this temperature, the flow-induced nucleation precursors are intrinsically unstable when the flow is stopped. Alfonso et al. investigated the flow-induced nucleation behavior in isotactic polypropylene[5] and isotactic poly(1-butene)[12] and reported that if the sheared sample is held quiescent at the pulling temperature for a sufficiently long time, it is possible to fully erase the memory of the flow field. Here we have proved that also i-PS behaves qualitatively in the same way. Sample C was sheared exactly as samples A and B, but it was held for 40 min at the shearing temperature before quenching. Neither WAXS nor SAXS patterns provide any evidence of order or orientation (Figure 6). This implies that the holding time was sufficient for the complete loss of the shear-induced structures through melting of the crystalline lamellar layers and relaxation of the oriented bundles of parallel chain segments.

Conclusions

The formation of nucleation precursors under the effect of the intense shear flow field has been demonstrated by spatially resolved simultaneous small- and wide-angle X-ray microdiffraction. Room temperature WAXS and SAXS patterns acquired from microvolumes in samples submitted to various thermal histories after application of an highly localized shear flow produced

by pulling a single fiber through a thin layer of molten i-PS provide strong evidence that ordered precursors are generated under flow also well above the melting point of crystals in quiescent conditions. At variance with analogous experiments performed on isotactic polypropylene, these precursors could be frozen by fast quenching and studied at room temperature due to the very low crystal growth rate of i-PS in the whole range of temperatures at which the polymer can crystallize.

The structuring produced at 260 °C by applying shear rates up to several hundred reciprocal seconds consists of the formation of a shish-kebab-type morphology whose geometrical characteristics strongly depend on the intensity of flow. Far from the fiber surface, a few tens of microns away where the flow field is less intense, the shish structures are made up by bundles of few parallel chains oriented along the flow direction. As foreseen by theory,[13] in line with the increase of the shear rate, the number of parallel chains forming the shish as well as the number of chain segments oriented along the flow direction increases moving toward the fiber surface. In addition, kebabs, consisting in layered lamellar assemblies, develop perpendicular to the shish.

Weak WAXS signals, corresponding to less than 1% crystallinity, have been detected in sampled microvolumes from which the meridian SAXS signal was also observed; this proves that the layered structures are crystalline. The long period of these structures is independent of distance from fiber surface, but the scattered intensity decreases in the same way as the crystallinity evaluated by WAXS does. This is very clear in the sample that has been quenched immediately after cessation of flow. A similar picture is also observed in the sample that was held for some time to crystallize at the temperature corresponding to maximum growth rate. In this case, however, relaxation of orientation and loss of segments from the oriented clusters leads to destruction of the smallest and less stable shish. Simultaneously, at the crystallization temperature, new nucleation events take place, together with the growth of crystals from the survived shear-induced nuclei, resulting in a gradual loss of average degree of orientation.

Finally, if the sample is held to relax at high temperature for sufficient time, all oriented nucleation precursors disappear, and the quenched system does not show any evidence of structural order even at location where the flow field was more intense.

Acknowledgment. M.C.G.G. is grateful to the European Community for the support of this research by a Marie Curie Fellowship of the European Community program "Improving Human Research Potential and the Socio-Economic Knowledge" under Contract HPMF-CT-2000-00892.

References and Notes

(1) Kumaraswamy, G.; Issaian, A. M.; Kornfield, J. A. *Macromolecules* **1999**, *32*, 7537.
(2) Somani, R. H.; Hsiao, B. S.; Nogales, A.; Srinivas, S.; Tsou, A. H.; Sics, I.; Baltá-Calleja, F. J.; Ezquerra, T. A. *Macromolecules* **2000**, *33*, 9385.
(3) Somani, R. H.; Hsiao, B. S.; Nogales, A.; Fruitala, H.; Srinivas, S.; Tsou, A. H. *Macromolecules* **2001**, *34*, 5902.
(4) Kumaraswamy, G.; Kornfield, J. A.; Yeh, F. J.; Hsiao, B. S. *Macromolecules* **2002**, *35*, 1762.
(5) Alfonso, G. C.; Scardigli, P. *Macromol. Chem. Phys., Macromol. Symp.* **1997**, *118*, 323.
(6) Varga, J.; Karger-Kocsis, J. *J. Polym. Sci., Part B: Polym. Phys.* **1996**, *34*, 657.
(7) Jay, F.; Haudin, J. M.; Monasse, B. *J. Mater. Sci.* **1999**, *34*, 2089.
(8) Somani, R. H.; Yang, L.; Hsiao, B. S. *Physica A* **2002**, *304*, 145.
(9) Li, L.; de Jeu, W. H. *Macromolecules* **2003**, *36*, 4862.
(10) Chai, C. K.; Dixon, N. M.; Gerrard, D. L.; Reed, W. *Polymer* **1995**, *36*, 661.
(11) Davey, R. J.; Liu, W.; Quayle, M. J.; Tiddy, G. J. T. *Cryst. Growth Des.* **2002**, *2*, 269.
(12) Alfonso, G. C.; Azzurri, F. In *Proceedings of the International Conference on Flow Induced Crystallization of Polymers*, Salerno, Italy, 2001.
(13) Ziabicki, A.; Alfonso, G. C. *Macromol. Chem. Phys., Macromol. Symp.* **2002**, *185*, 211.
(14) Riekel, C. *Rep. Prog. Phys.* **2000**, *63*, 233.
(15) Monasse, B. *J. Mater. Sci.* **1992**, *27*, 6047.
(16) Suzuki, T.; Kovacs, A. J. *Polym. J.* **1970**, *1*, 82.
(17) Taguchi, K.; Miyaji, H.; Izumi, K.; Hoshino, A.; Miyamoto, Y.; Kokawa, R. *J. Macromol. Sci., Part B: Phys.* **2002**, *41*, 1033.
(18) Hammersley, A. Web site: http://www.esrf.fr/computing/expg/subgroups/ data_analysis/FIT2D/index/html.
(19) Natta, G.; Corradini, P.; Bassi, I. W. *Nuovo Cimento* **1960**, *15*, 68.
(20) Samon, J. M.; Schultz, J. M.; Hsiao, B. S.; Seifert, S.; Stribeck, N.; Gurke, I.; Collins, G.; Saw, C. *Macromolecules* **1999**, *32*, 8121.
(21) Somani, R. H.; Yang, L.; Hsiao, B. S.; Agarwal, P. K.; Fruitwala, H. A.; Tsou, A. H. *Macromolecules* **2002**, *35*, 9096.
(22) Petermann, J.; Gleiter, H. *Polym. Lett. Ed.* **1977**, *15*, 649.
(23) Petermann, J.; Gohil, R. M. *Polym. Lett. Ed.* **1980**, *18*, 781.
(24) Lemstra, P. J.; Kooistra, T.; Challa, G. *J. Polym. Sci., Part A-2* **1972**, 823.
(25) Gu, F.; Bu, H.; Zhang, Z. *Macromolecules* **2000**, *33*, 5490.

MA0350157